Thermo-economic performance optimization of a grid-connected, solar-powered building with hydrogen-based energy storage, including epistemic and aleatory uncertainty quantification

Diederik Coppitters[a,b,c], Ward De Paepe[d] and Francesco Contino[e]

[a] *Thermal Engineering and Combustion Unit, University of Mons (UMONS), Place du parc 20, 7000 Mons, Belgium, diederik.coppitters@umons.ac.be, CA*

[b] *Fluid and Thermal Dynamics (FLOW), Vrije Universiteit Brussel, Pleinlaan 2, 1050 Brussels, Belgium*

[c] *Combustion and Robust Optimization Group (BURN), Vrije Universiteit Brussel (VUB) and Université Libre de Bruxelles (ULB), 1050 Brussels, Belgium*

[d] *Thermal Engineering and Combustion Unit, University of Mons (UMONS), Place du parc 20, 7000 Mons, Belgium, ward.depaepe@umons.ac.be*

[e] *Institute of Mechanics, Materials and Civil Engineering (iMMC), Université catholique de Louvain (UCLouvain), Place du Levant, 2, 1348 Louvain-la-Neuve, Francesco.contino@uclouvain.be*

Abstract:

Combining battery systems and hydrogen-based energy systems provides viable support for intermittent renewable energy sources to cover the energy demand continuously. During the planning of such a hybrid renewable energy system, the model parameters are generally fixed or their uncertainty is bundled into a precise distribution, leading to a representation that does not distinguish between uncertainty related to natural variation (i.e. aleatory uncertainty) and uncertainty related to a lack of data (i.e. epistemic uncertainty). Therefore, after a stochastic evaluation, the designer is unable to determine if the uncertainty on the objective is reducible by gaining more knowledge or if external measures are required (e.g. government-induced stabilization plan for the gas price). To assess these limitations on a grid-connected household supported by batteries and hydrogen storage, we characterized the parameters with parametric probability-boxes. Thereafter, we performed a global sensitivity analysis through a novel computationally-efficient uncertainty quantification method. This paper provides the main drivers of the variation in levelized cost of exergy for typical designs and illustrates the effect of epistemic uncertainty on these drivers. Results show that the epistemic uncertainty dominates the levelized cost of exergy variation for a photovoltaic array alone. Therefore, increased data collection is required on the gas price and electricity price evolution. For a photovoltaic array with battery stack, the uncertainty on the gas price is the dominant driver of the levelized cost of exergy variation. With additional hydrogen-based storage, the interest rate is the dominant driver and it proves robust towards epistemic uncertainty. Hence, more demonstration projects are required to reduce mainly the natural variation of the interest rate. Future work will integrate this uncertainty quantification into a robust optimization framework.

Keywords:

Energy storage, Global Sensitivity Analysis, Levelized cost of energy, Probability box, Uncertainty quantification.

1. Introduction

Solar PhotoVoltaic (PV) systems dominate the renewable capacity growth [1]. Nevertheless, PV systems are unable to cover the entire energy demand, due to the intermittent behavior of solar energy. To perform intermittent balancing, battery energy storage (from days to weeks) and hydrogen energy storage (from weeks to months) provide a flexible, adequate technology [2]. Studies on such Hybrid

Renewable Energy Systems (HRES) are well-established. Lacko et al. evaluated Combined Heat and Power (CHP) generation for a standalone household based on three renewable-inspired system configurations and conclude that an entire renewable energy supply is both feasible and more cost-efficient than integrating a fossil heat supply [3]. Özgirgin et al. concluded that a PEM fuel cell with a PV system is a viable solution for stand-alone household in a CHP configuration [4]. Zafar et al. illustrated that a residential building powered by PV, wind turbine and electrolyzer-tank-fuel cell achieves improved energy and exergy efficiency when the heat is also used to cover the demand [5].
Despite that these studies indicate the potential of batteries and hydrogen-based energy storage in a CHP application, the design parameters are generally fixed, regardless of what will happen in reality. This can result in suboptimal designs. In the rare studies including uncertainties, the applications are limited to a vague uncertainty characterization (e.g. assuming uniform distribution with generic range), leading to inaccurate conclusions. By bundling the uncertainty into a precise distribution, the representation does not distinguish between uncertainty related to natural variation (i.e. aleatory uncertainty) and uncertainty related to lack of data (i.e. epistemic uncertainty). Therefore, after a stochastic evaluation, the designer is left clueless if the uncertainty is due to the actual variation of the parameter, or if it is mainly driven by the lack of data on those parameters, and therefore cannot take appropriate actions. To assess these limitations on a grid-connected household supported by batteries and hydrogen storage, we first characterized the significant parameters through precise distributions and parametric probability-boxes [6]. This characterization leads to a clear distinction between the uncertainties related to the lack of information and uncertainties related to natural variation. Thereafter, we performed Uncertainty Quantification (UQ) on the Levelized Cost Of eXergy (LCOX). Finally, we performed a global sensitivity analysis to clarify the origin of the variation of the LCOX, leading to clear actions for the designer to reduce the sensitivity towards uncertainty.

2. Method

In this section, the HRES is described and the system objective is introduced. Thereafter, the characterization of the uncertainties on the model parameters is provided, followed by the UQ method to propagate these uncertainties.

2.1. Hybrid Renewable Energy System (HRES) model

The considered system is a household connected to the power grid and gas grid, supported by a HRES (Figure 1). Since a study on the self-sufficiency is not the main purpose of the paper, the power and gas grid are considered permanently available and able to cover the demand. The HRES consists of a PV array, which is coupled to a DC bus bar through a DC-DC converter with Maximum Power Point Tracking. We integrated a battery stack and electrolyzer array with storage tank to store the excess of PV array electricity. A fuel cell array is implemented to produce power and heat from the stored hydrogen.

2.1.1. Component models

To determine the electricity produced by a PV array, we imported the experimentally-validated model out of the PVlib Python library [7]. The current-voltage characteristic of the PV array is quantified through the following single-diode equation:

$$I_{\mathrm{PV}} = I_{\mathrm{L}} - I_0 \left(\exp \left(\frac{U + I R_{\mathrm{s}}}{n_{\mathrm{diode}} N_{\mathrm{s}} U_{\mathrm{th}}} \right) - 1 \right) - \frac{U + I R_{\mathrm{s}}}{R_{\mathrm{sh}}}. \tag{1}$$

The parameters in Equation 1 are not accessible through manufacturer data. Therefore, we characterized these parameters via the method presented by De Soto et al. [8].
To store PV excess power, we selected the lead-acid battery technology in the HRES. To characterize the performance of a lead-acid battery stack, we adopted the experimentally-validated model of

Blaifi et al. [9]. The general voltage-current relation for a lead-acid battery is defined as:

$$U_{\mathrm{bat}} = U_{\mathrm{bat,oc}} + I_{\mathrm{bat}} R_{\mathrm{bat}}, \tag{2}$$

where the current I_{bat} is positive during charge and negative during discharge. The resistance R_{bat} depends on temperature, current magnitude and capacity. We refer to Blaifi et al. for the detailed quantification of these parameters [9]. The State Of Charge (SOC) is the fraction of the total capacity stored in the battery:

$$\mathrm{SOC}\,(t) = \mathrm{SOC}_0 + \frac{1}{C\,(t)} \int_0^t \eta_{\mathrm{bat}}\,(t)\, I\,(t)\, \mathrm{d}t, \tag{3}$$

We estimated the lifetime based on SOC variations through the commonly implemented Rainflow cycles counting method [10]. To avoid excessive reduction of the lifetime and active mass losses due to gassing effects, overcharging and overdischarging are avoided, while the maximum charge current and maximum discharge current are limited to $C_{\mathrm{nom}}/10$ and $C_{\mathrm{nom}}/3.3$, respectively [11].
In addition to the battery stack to consume excess of PV array electricity, we selected a Proton Exchange Membrane (PEM) electrolyzer for its fast response time (<1 s) and full load flexibility ($0\,\%$ - $100\,\%$) [12]. To determine the voltage-current characteristic, efficiency and hydrogen flow rate, we selected the experimentally-validated model from Abdin et al. [13]. The operating voltage is characterized according to the following equation:

$$U_{\mathrm{EL}} = U_{\mathrm{EL,oc}} - U_{\mathrm{EL,act}} - U_{\mathrm{EL,ohm}} - U_{\mathrm{EL,con}}. \tag{4}$$

We refer to Abdin et al. for further details on the determination of the overpotentials [13]. Finally, following the working point of the electrolyzer array, the hydrogen molar flow rate $n_{\mathrm{H_2}}$ is formulated as:

$$n_{\mathrm{H_2}} = \frac{I}{2F}. \tag{5}$$

The pressurized hydrogen produced in the electrolyzer is stored in a storage tank. Filling up the storage tank increases the tank pressure, until the electrolyzer outlet pressure is reached, according to the ideal gas law [14]:

$$p_{\mathrm{t}} - p_{\mathrm{t,init}} = Z \frac{N_{\mathrm{H_2}} R_{\mathrm{u}} T_{\mathrm{t}}}{M_{\mathrm{H_2}} V_{\mathrm{t}}}. \tag{6}$$

The compressibility factor Z for H_2 is equal to 1 at moderate pressure (<$100\,\mathrm{bar}$) [14].
To generate electricity by converting hydrogen and oxygen into water, we selected a PEM fuel cell. The PEM fuel cell is a widespread commercial technology, which operates at low operational temperature ($70\,°\mathrm{C}$- $100\,°\mathrm{C}$) and achieves high power densities (up to $2\,\mathrm{W/cm^2}$). To represent this conversion of hydrogen and oxygen into water, we adopted the model from Murugesan et al. which is experimentally validated on the Ballard-Mark-V PEM fuel cell [15]. The operating current depends on the converted hydrogen molar flow rate:

$$I_{\mathrm{FC}} = 2F n_{\mathrm{FC,H_2}}. \tag{7}$$

The electric potential produced during water composition out of hydrogen and oxygen is equal to the Nernst potential minus the losses:

$$U_{\mathrm{FC}} = U_{\mathrm{FC,Nernst}} - U_{\mathrm{FC,act}} - U_{\mathrm{FC,ohm}} - U_{\mathrm{FC,con}}. \tag{8}$$

We refer to the work of Murugesan et al. for the detailed quantification of these losses [15].

2.1.2. Climate and demand data

The considered location to evaluate the HRES performance is Brussels (Belgium). A Typical Meteorological Year is used to represent the hourly climate data over a year (yearly irradiance: $1118\,\mathrm{kWh/year}$, average ambient temperature: $10.7\,°\mathrm{C}$) [16]. To characterize the effect of the load on the performance of the HRES, a dwelling demand is adopted (electricity demand: $3.98\,\mathrm{MWh/year}$, heat demand: $20.81\,\mathrm{MWh/year}$). Since the demand behavior depends on both climate conditions and human behavior, we adopted the method presented by Montero Carerro et al. to adapt the demand profiles to the climate and behavior in Belgium [17].

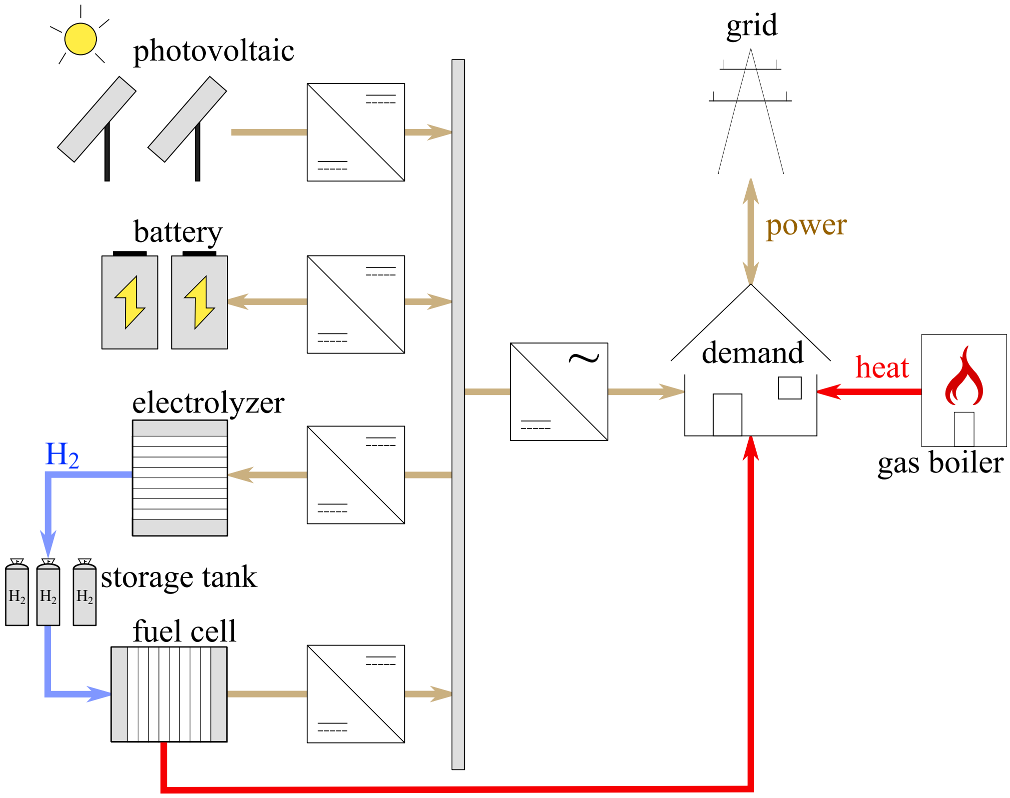

Figure 1: Schematic of the system

2.2. Design parameters, objective and indicator

The capacity of the PV array, battery stack, PEM electrolyzer, PEM fuel cell and storage tank are selected as design parameters. By considering the capacities as independent design parameters, the optimization algorithm can exclude any technology (e.g. set the battery stack capacity to $0\,\mathrm{kWh}$). Nonetheless, large system capacities induce large investment, operating and replacement costs. Therefore, minimizing the Levelized Cost Of eXergy (LCOX) is defined as the system objective. The LCOX reflects the system cost per unit of exergy covered [18]:

$$\mathrm{LCOX} = \frac{\mathrm{CAPEX_a} + \mathrm{OPEX_a} + C_{\mathrm{r,a}} + C_{\mathrm{e,a}} - C_{\mathrm{e,a,sold}} + C_{\mathrm{g,a}}}{\sum_{i=1}^{8760} X_{\mathrm{load}}}. \tag{9}$$

To determine the annual system cost, the annualized investment cost $\mathrm{CAPEX_a}$, operational cost $\mathrm{OPEX_a}$, replacement cost $C_{\mathrm{r,a}}$, grid electricity cost $C_{\mathrm{e,a}}$, electricity sold to the grid at wholesale price $C_{\mathrm{e,a,sold}}$ and gas cost $C_{\mathrm{g,a}}$ are added together. We refer to Zakeri et al. for the detailed quantification of these parameters [18]. When the cost parameters are quantified, the LCOX is defined by dividing the annual system cost by the total required exergy X_{load}. The required exergy by the demand is equal to the sum of the electricity demand X_{elec} and the exergy content of the heat demand X_{heat}, which corresponds to the heat energy demand corrected by the Carnot coefficient [19]. Additionally, the Self-sufficiency ratio in terms of eXergy (SSX) is defined as the amount of exergy covered by the HRES, divided by the total required exergy. The SSX is an indicator for adopters of the HRES, as it illustrates the resilience against large electricity/gas price increases and the protection against power cuts, which are more likely in the future [20]. Consequently, for this system, the performance is determined by the LCOX, at different SSX thresholds. As the SSX is a model output, the different

Table 1: P-box input parameters. The parameters indicated by $\%$ refer to the total variation based on the reference dataset. $\%_{\mathrm{irradiance}} =$ percentage of yearly average solar irradiance, $\%_{\mathrm{demand,elec}} =$ percentage of yearly average electricity demand, $\%_{\mathrm{demand,heat}} =$ percentage of yearly average heat demand, $C_{\mathrm{elec}} =$ wholesale average grid electricity price, $C_{\mathrm{heat}} =$ average gas price.

parameter	mean, μ	standard deviation, σ	unit	Ref.
$\%_{\mathrm{irradiance}}$	[93.1,98.2]	[2.9,6.9]	$\%$	[16]
$\%_{\mathrm{demand,elec}}$	[103.2,111.0]	[2.3,9.1]	$\%$	[23]
$\%_{\mathrm{demand,heat}}$	[82.9,99.4]	[2.9,19.2]	$\%$	[24]
C_{elec}	[59.9,84.1]	[15.2,33.8]	€/MWh	[23]
C_{heat}	[36.5,48.5]	[7.1,16.5]	€/MWh	[25, 26]
inflation	[0.88,1.79]	[0.90,1.58]	$\%$	[27]

SSX of interest cannot be imposed directly into the model. Instead, to acquire the optimized LCOX in function of the SSX indirectly, maximizing the SSX is selected as a second optimization objective in a bi-objective optimization framework. Ultimately, the resulting set of optimized designs form a Pareto front for each demand type, which corresponds to a function of the LCOX with respect to the SSX. To produce this Pareto front, the Nondominated Sorting Genetic Algorithm (NSGA-II) algorithm is applied, which is a multi-objective genetic algorithm, suitable for optimization of complex, non-linear models [21, 22].

2.3. Uncertainty quantification

The design, planning and operation of the HRES are subject to uncertainty. This uncertainty is characterized by the natural variation of the parameter (i.e. aleatory uncertainty) and the lack of information (i.e. epistemic uncertainty). We consider the parameters related to investment (i.e. investment cost, replacement cost, interest rate) subject to epistemic uncertainty only, as these parameters can be fully characterized by gaining knowledge (e.g. a thorough market study) and they do not evolve over time. This epistemic uncertainty is represented by a precise probability, in the form of a Uniform distribution. The parameters subject to variation over the lifetime of the HRES (the grid electricity and gas price, heat and electricity demand, inflation rate and solar irradiance) are subject to both epistemic and aleatory uncertainty: In addition to the lack of knowledge on their average value, the evolution of these parameters over time is inherently unpredictable and therefore subject to a natural, irreducible variation (i.e. political decisions on the future energy mix will define the grid electricity price evolution). Therefore, a parametric probability-box (p-box) is used to characterize the epistemic and aleatory uncertainty on each of these parameters. While a precise probability is characterized by fixed statistical moments, a p-box is defined by a range on the mean μ and standard deviation σ instead: $\mu \in [\underline{\mu}, \overline{\mu}]$, $\sigma \in [\underline{\sigma}, \overline{\sigma}]$. Hence, a p-box is defined by a lower and upper bound Cumulative Distribution Function F_X (CDF): $\underline{F}_X(x) \leq F_X(x) \leq \overline{F}_X(x)$. Consequently, any CDF of the underlying parametric family that lies between the bounds represents a possible distribution for the uncertain parameter. Conclusively, the distribution family represents the aleatory uncertainty of each parameter, while the range of the statistical moments represents the epistemic uncertainty.

To construct the parametric p-boxes, the bounds should be properly characterized. When no expert knowledge or physical reasons are available to set these bounds, a feasible method is to determine the bounds based on a confidence level. Assuming a Uniform prior on the statistical moments of a Gaussian distribution, the confidence bounds are quantified on a set of predictions for each parameter based on the method by Schöbi et al. [6]. To illustrate, six predictions on the wholesale electricity price for 2030 in Belgium (base case scenario, decentral scenario and large scale renewable energy system scenario, each determined in the coal-before-gas merit order and gas-before-coal merit order) are used to quantify the bounds for the grid electricity price based on a $95\,\%$ confidence level [23]. The resulting ranges for the p-boxes are presented in Table 1, as well as the references for the corresponding datasets.

To propagate the uncertain parameters through the system model and evaluate their effect on the LCOX, we considered a computationally efficient sparse PCE method [28]. While this sparse PCE method is well-defined for precise probability distributions, we adapted this method to propagate p-boxes, based on the method developed by Schöbi et al. [6].

3. Results and discussion

In the results section, the Pareto front is described that illustrates the trade-off between minimizing the LCOX and maximizing the SSX when a deterministic design optimization is performed (i.e. no uncertainty). Then, out of these optimized designs, 4 representative designs are selected and are subjected to uncertainty on the input. The resulting p-boxes of the LCOX are discussed and a global sensitivity analysis is performed on these 4 designs, in order to illustrate the effect of epistemic and aleatory uncertainty on the LCOX.

3.1. Levelized cost of exergy in function of self-sufficiency

To determine a set of optimized designs, a deterministic optimization is performed, aiming to minimize the LCOX and maximize the SSX. As no uncertainty is considered in this optimization, average values of the uniform distributions and average values of the mean for the p-boxes are selected for the parameters. Due to the trade-off between minimizing the LCOX and maximizing the SSX, the Pareto front provides designs with an optimized LCOX for different levels of SSX. Clearly, at low SSX (18 % - 21 %), designs with a PV array alone (i.e. PV-designs) result in the lowest LCOX (Figure 2). As such designs lack the possibility of energy storage and heat production, the maximum attained SSX of PV-designs is limited. Therefore, to reach the next SSX threshold (up to 55 %), at the expense of minimal increase in LCOX, a PV array with battery stack (i.e. PV-battery designs) is constructed by the optimization algorithm. To reach the optimal SSX (>55 %) at optimized LCOX, batteries are gradually replaced by the hydrogen-based energy system, to cover part of the heat demand with the HRES as well. Conclusively, 4 different types of HRES are found to reach optimized LCOX in function of the SSX: a PV-design, a PV-battery design, a PV-battery-hydrogen design and a PV-hydrogen design.

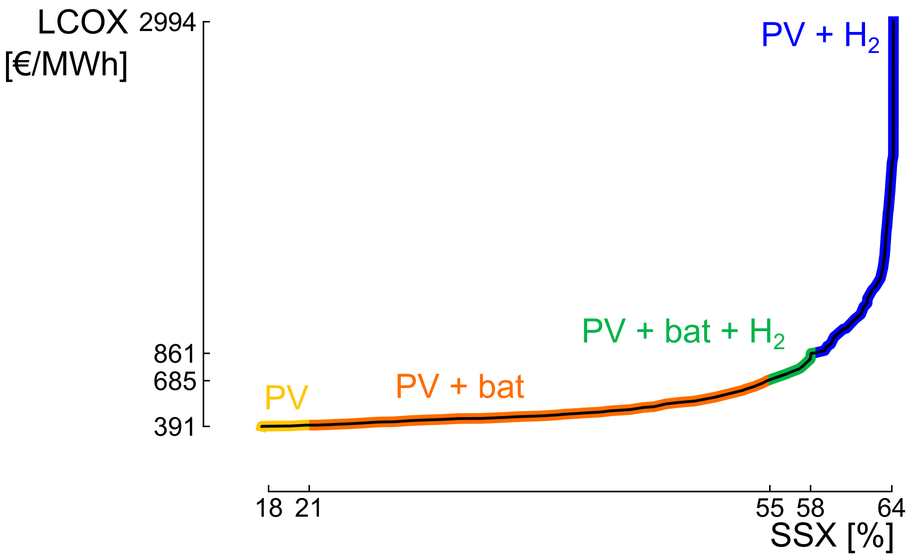

Figure 2: The optimal designs on the Pareto front illustrate the trade-off between minimizing the Levelized Cost Of eXergy (LCOX) and maximizing the eXergy Self-Sufficiency ratio (SSX). A photovoltaic array achieves the lowest LCOX. Improving the SSX is first done by including a battery stack, followed by a hydrogen-based system. Finally, to attain optimal SSX, the battery stack is replaced by a hydrogen-based energy system to further increase the self-sufficiency in terms of heat demand.

Table 2: Typical PV-design (PV), PV-battery design (PV + bat), PV-battery-hydrogen design (PV + bat + H_2) and PV-hydrogen design (PV + H_2) which achieve optimized Levelized Cost Of eXergy (LCOX) at different levels of Self-Sufficiency ratio for eXergy (SSX).

type	design characteristics					deterministic		uncertain	
	N_{PV}	N_{Bat}	N_{ELEC}	N_{FC}	N_{tank}	LCOX	SSX	μ_{LCOX}	σ_{LCOX}
	$\mathrm{kW_p}$	kWh	kW	kW	kWh	€/MWh	%	€/MWh	€/MWh
PV	2.7					389.5	17.5	[344.9,440.8]	[13.9,32.2]
PV + bat	5.0	2.2				411.8	24.8	[375.3,465.5]	[15.5,31.9]
PV + bat + H_2	42.1	17.8	0.6	1.0	247.1	823.8	57.9	[752.5,1008.9]	[62.1,97.8]
PV + H_2	35.5		4.1	1.0	828.7	878.4	59.1	[811.4,1016.3]	[54.1,84.9]

3.2. Uncertainty Quantification

Out of the deterministic design optimization performed in subsection 3.1., 4 designs are extracted with different HRES characteristics (a PV-design, PV-battery design, PV-battery-hydrogen design and PV-hydrogen design, characterized in Table 2) and the uncertainties are propagated through these 4 designs. Due to the combination of Uniform distributions and p-boxes at the model input, the resulting LCOX is determined by a p-box. When comparing the PV-design with the PV-battery design, the range on the mean and standard deviation of the LCOX illustrate that the PV-battery design is slightly less sensitive to epistemic uncertainty, despite the slightly higher average mean LCOX value (Figure 3 and Table 2). The difference in mean LCOX is attributed to the higher HRES capacity of the PV-battery design, which induces higher investment and replacement cost. On the other side, the reduced sensitivity on epistemic uncertainty is clarified by the reduced dependency on the electricity grid and thus reduced dependency on the electricity price, which carries large epistemic uncertainty.
The PV-battery-hydrogen design and PV-hydrogen design, which operate at high SSX ($57.9\,\%$ and $59.1\,\%$ respectively), are more sensitive to epistemic uncertainty than the PV-design and PV-battery design. In between the PV-hydrogen design and PV-battery-hydrogen design, the former is clearly less sensitive to epistemic uncertainty than the latter. As the explanation of this result is not straightforward, a global sensitivity analysis is performed in the next section, to study the origin of the LCOX variation for these designs.

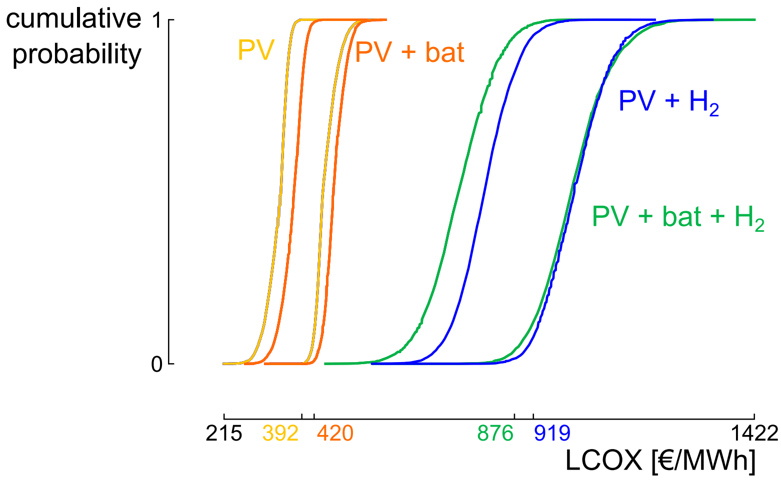

Figure 3: The probability boxes of the different designs illustrate that the PV-battery-hydrogen design and PV-hydrogen design operate at higher Levelized Cost Of eXergy (LCOX), as opposed to the PV-design and PV-battery design. Nevertheless, the PV-hydrogen design is clearly less sensitive to epistemic uncertainty than the PV-battery-hydrogen design, which is represented by the distance between the p-box bounds.

3.3. Global sensitivity analysis

In this section, a global sensitivity analysis is performed on the 4 designs. In a global sensitivity analysis with precise distributions, sensitivity indices are produced which indicate the contribution of each

parameter uncertainty to the variance of the objective. As in this work p-boxes are considered to characterize the uncertainty of part of the parameters at the model input, the resulting sensitivity indices are characterized by a range of values. The average sensitivity index value indicates the importance of the aleatory parameter uncertainty to the LCOX variance, while the range on the sensitivity index indicates the level of confidence on the sensitivity index due to the global epistemic uncertainty [6].
The sensitivity indices computed for the PV-design illustrate that the uncertainty on the achieved LCOX is dominantly driven by the uncertainty on the gas price and electricity price (Figure 4). This follows out of the large dependency on the electricity grid and gas grid to cover the demand in this design (SSX = $17.5\,\%$). Due to the significant epistemic uncertainty, it remains uncertain which aleatory parameter uncertainty is the main driver of the LCOX variability, i.e. the contribution of the aleatory uncertainty on the gas price to the variation of the LCOX lies between $31.0\,\%$ and $93.6\,\%$, while the contribution of the aleatory uncertainty on the electricity price lies between $5.0\,\%$ and $64.8\,\%$. Hence, gaining additional knowledge (e.g. additional predictions) to reduce the epistemic uncertainty is the main action suggested for this PV-design, in order to reduce the overall uncertainty on the LCOX.

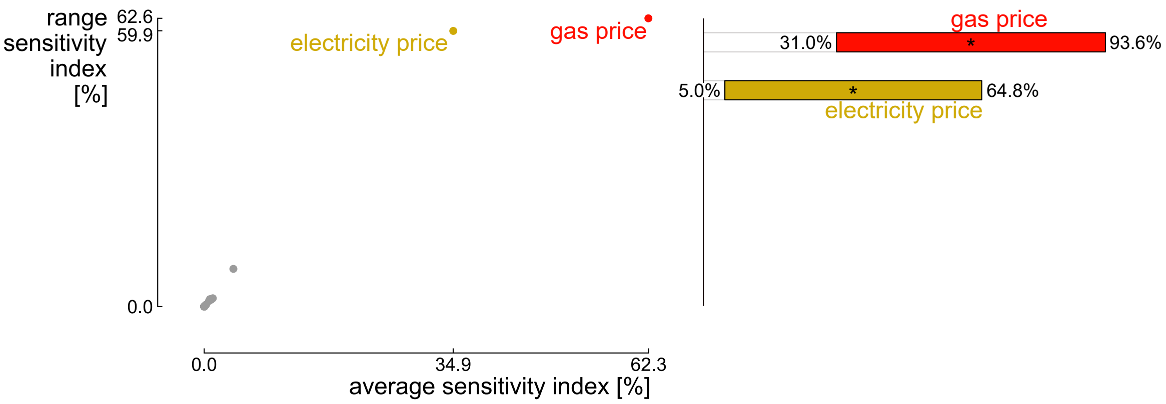

Figure 4: For the PV design, the contribution of the uncertainty related to the gas price towards the variability of the Levelized Cost Of eXergy (LCOX) is the highest on average. However, the large range on the sensitivity indices indicates the significant effect of the epistemic uncertainty.

The variation in the LCOX achieved by the PV-battery design will always be dominated by the gas price uncertainty, as there is no overlap between the gas price and electricity price sensitivity index ranges (Figure 5). Hence, despite the significant epistemic uncertainty, the aleatory uncertainty related to the gas price is identified as the main driver. Therefore, external measures to reduce this aleatory uncertainty, such as gas price stabilization plans from the government, are suggested as the most efficient measures to improve the LCOX robustness for this design. Due to the increased self-sufficiency for electricity (i.e. reduced dependency on the electricity grid) as opposed to the PV-design, the average impact of the uncertainty from the electricity price on the LCOX variation is reduced. Instead, due to the inclusion of a battery stack, the uncertainty of the battery lifetime gains importance. Additional information should be gained to reduce the overall epistemic uncertainty, in order to determine if the electricity price or battery lifetime aleatory uncertainty is the most significant driver of the LCOX uncertainty.
For the PV-battery-hydrogen design, the contribution is spread over different parameters (Figure 6). Clearly, the design remains sensitive to the uncertainty on the grid electricity price, despite the low dependency on the grid to cover the electricity demand. This follows out of the fact that this design sells a large amount of excess solar energy to the grid. However, due to the significant installed capacity (and thus investment cost), the uncertainty on the interest rate gains importance, and the sensitivity index proves to be robust towards the global epistemic uncertainty (ranges between $16.6\,\%$ and $32.9\,\%$). Therefore, the focus should be to reduce the aleatory uncertainty of the interest rate (e.g. by additional demonstration projects) and to increase the data collection on the electricity price evolution.

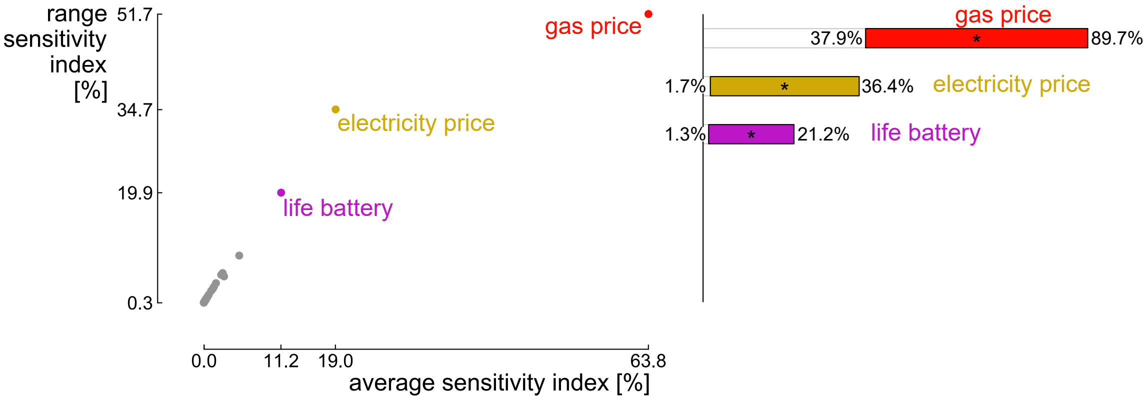

Figure 5: Despite the epistemic uncertainty, the uncertainty on the gas price is the dominant contributor to the variability of the Levelized Cost Of eXergy (LCOX) for the PV-battery design.

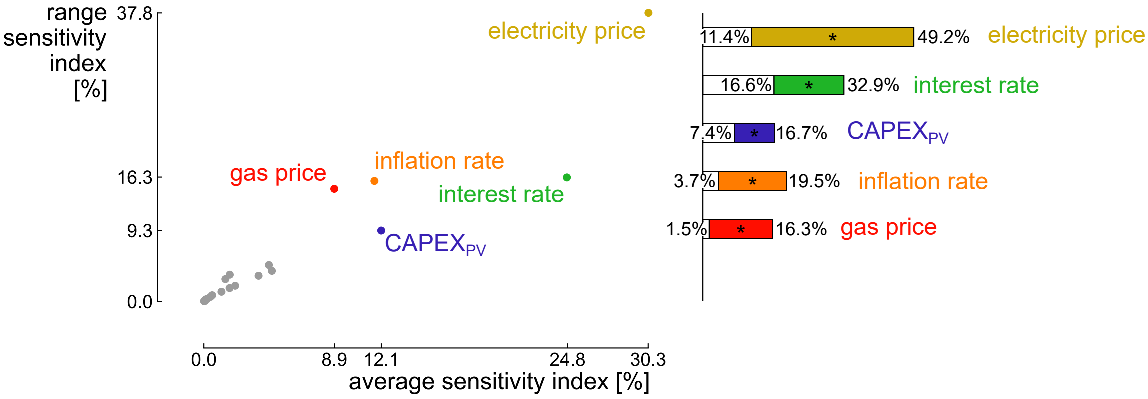

Figure 6: For the PV-battery-hydrogen design, the contribution is spread over different parameters. Clearly, the importance of the uncertainty related to the electricity price is the most sensitive towards epistemic uncertainty.

The increased capacity, and hence increased significance of the uncertainty on the interest rate largely defines the LCOX variation of the PV-hydrogen design (Figure 7). The uncertainty on the interest rate is significantly more important than the other parameters, while its importance proves to be more robust for the epistemic uncertainty than the importance of the uncertainty related to the electricity price. To clarify, the actual uncertainty of the electricity price might be as low as $6.0\,\%$, while the importance of the uncertainty related to the interest rate will be at least $24.4\,\%$. Consequently, as the LCOX variation is largely defined by the uncertainty on the interest rate, the actual sensitivity towards epistemic uncertainty of this design is lower than for the PV-battery-hydrogen design, as illustrated in Figure 3.

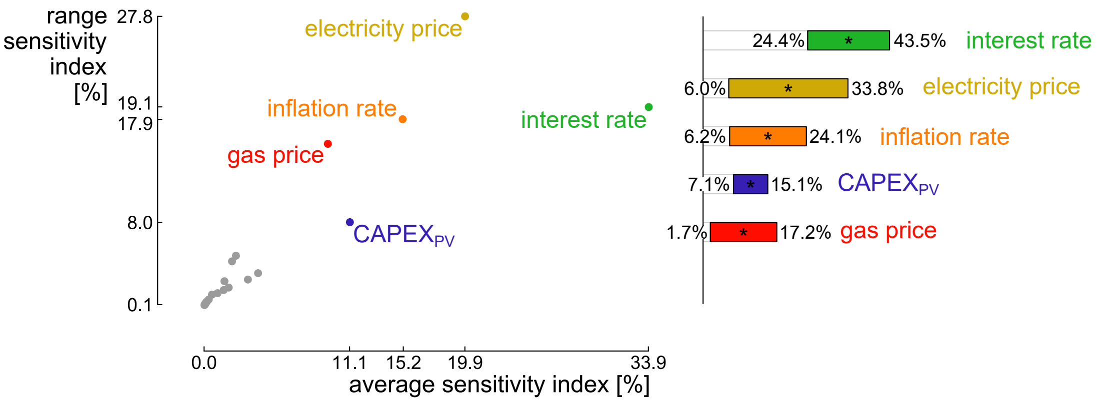

Figure 7: For the PV-hydrogen design, the uncertainty on the interest rate dominates the Levelized Cost Of eXergy (LCOX) variation and proves more robust towards epistemic uncertainty than the electricity price.

For the evaluated designs, parameters such as the heat demand, electricity demand and solar irradiance have a low average sensitivity index ($\leq 5\,\%$) and a low sensitivity index range ($\leq 5\,\%$). Therefore, these parameters can be considered as unimportant contributors to the LCOX variation and no further data acquisition is effective to reduce the LCOX variation.

4. Conclusion

For a grid-connected household, supported by a hybrid renewable energy system including photovoltaics, batteries and hydrogen-based energy system, optimizing the levelized cost of exergy for different exergy self-sufficiency ratio thresholds brings forward 4 typical designs (in increasing order of exergy self-sufficiency ratio): a photovoltaic array alone ($17.5\,\%$), photovoltaics with battery stack ($24.8\,\%$), photovoltaics with battery stack and hydrogen-based energy storage ($57.9\,\%$) and finally photovoltaics with large hydrogen-based energy storage ($59.1\,\%$).
For the photovoltaic array alone, the variation on the levelized cost of exergy is mainly driven by the epistemic uncertainty related to the gas price and the electricity price. Therefore, increasing the data collection on these parameters is suggested as the main action to reduce the variance of the levelized cost of electricity.
For a photovoltaic array with battery stack, the exergy self-sufficiency is higher, resulting in reduced dependency on the electricity grid and thus reduced impact of the electricity price on the levelized cost of exergy variation. Therefore, for this design, the main action is to improve the understanding of the gas price evolution (and thus reduce its aleatory uncertainty), as it is the dominant driver of the levelized cost of exergy variation, despite the remaining large effect of epistemic uncertainty (i.e. gas price importance ranges between $37.9\,\%$ and $89.7\,\%$).
The aleatory uncertainty related to the gas price is identified as the main driver of the PV-battery design. Therefore, external measures to reduce this aleatory uncertainty, such as gas price stabilization plans from the government, are suggested as the most efficient measures to improve the LCOX robustness for this design. The variation of the levelized cost of exergy for a photovoltaic array with battery stack and hydrogen-based energy storage is significantly driven by the interest rate. While its importance proves robust towards epistemic uncertainty, the importance of the uncertainty of the electricity price for this design lies between $11.4\,\%$ and $49.2\,\%$. Hence, actions should be undertaken to gain data on the evolution of the electricity price, while for the interest rate, reducing the aleatory uncertainty of the interest rate by introducing more demonstration projects provides is suggested.
For the photovoltaic array with large hydrogen storage, the interest rate dominates the levelized cost of exergy, due to the large system capacity and thus large investment and replacement costs. Therefore, like for the previous design, reducing the natural variation of the interest rate is required, while further data collection on gas price and inflation rate is only of minor importance to reduce the levelized cost of exergy variation.
Future work will focus on the integration of this uncertainty quantification into a robust design optimization framework.

Acknowledgments

The first author acknowledges the support of Fonds de la Recherche Scientifique - FNRS [35484777 FRIA-B2].

References

[1] "Renewables 2018: Market analysis and forecast from 2018 to 2023," International Energy Agency, Tech. Rep., 2018.

[2] M. Aneke and M. Wang, "Energy storage technologies and real life applications–A state of the art review," *Applied Energy*, vol. 179, pp. 350–377, 2016.

[3] R. Lacko, B. Drobnič, M. Mori, M. Sekavčnik, and M. Vidmar, "Stand-alone renewable combined heat and power system with hydrogen technologies for household application," *Energy*, vol. 77, pp. 164–170, 2014.

[4] E. Özgirgin, Y. Devrim, and A. Albostan, "Modeling and simulation of a hybrid photovoltaic (PV) module-electrolyzer-PEM fuel cell system for micro-cogeneration applications," in *International Journal of Hydrogen Energy*, vol. 40, no. 44, 2015, pp. 15 336–15 342.

[5] S. Zafar and I. Dincer, "Energy, exergy and exergoeconomic analyses of a combined renewable energy system for residential applications," *Energy and Buildings*, vol. 71, pp. 68–79, 2014.

[6] R. Schöbi and B. Sudret, "Global sensitivity analysis in the context of imprecise probabilities (p-boxes) using sparse polynomial chaos expansions," *Reliability Engineering & System Safety*, vol. 187, pp. 129–141, 2019.

[7] W. F. Holmgren, C. W. Hansen, and M. A. Mikofski, "pvlib python: a python package for modeling solar energy systems," *The Journal of Open Source Software*, vol. 3, p. 884, 2018.

[8] W. De Soto, S. A. Klein, and W. A. Beckman, "Improvement and validation of a model for photovoltaic array performance," *Solar Energy*, vol. 80, no. 1, pp. 78–88, 2006.

[9] S. Blaifi, S. Moulahoum, I. Colak, and W. Merrouche, "An enhanced dynamic model of battery using genetic algorithm suitable for photovoltaic applications," *Applied Energy*, vol. 169, pp. 888–898, may 2016.

[10] R. Dufo-López, J. M. Lujano-Rojas, and J. L. Bernal-Agustín, "Comparison of different lead–acid battery lifetime prediction models for use in simulation of stand-alone photovoltaic systems," *Applied Energy*, vol. 115, pp. 242–253, 2014.

[11] C. Phurailatpam, B. S. Rajpurohit, and L. Wang, "Planning and optimization of autonomous DC microgrids for rural and urban applications in India," *Renewable and Sustainable Energy Reviews*, vol. 82, pp. 194–204, feb 2018.

[12] A. Buttler and H. Spliethoff, "Current status of water electrolysis for energy storage, grid balancing and sector coupling via power-to-gas and power-to-liquids: A review," *Renewable and Sustainable Energy Reviews*, vol. 82, pp. 2440–2454, 2018.

[13] Z. Abdin, C. J. Webb, and E. M. Gray, "Modelling and simulation of a proton exchange membrane (PEM) electrolyser cell," *International Journal of Hydrogen Energy*, vol. 40, no. 39, pp. 13 243–13 257, oct 2015.

[14] H. Görgün, "Dynamic modelling of a proton exchange membrane (PEM) electrolyzer," *International Journal of Hydrogen Energy*, vol. 31, no. 1, pp. 29–38, 2006.

[15] K. Murugesan and V. Senniappan, "Investigation of water management dynamics on the performance of a Ballard-Mark-V proton exchange membrane fuel cell stack system," *Int. J. Electrochem. Sci*, vol. 8, pp. 7885–7904, 2013.

[16] T. Huld, R. Müller, and A. Gambardella, "A new solar radiation database for estimating PV performance in Europe and Africa," *Solar Energy*, vol. 86, no. 6, pp. 1803–1815, jun 2012.

[17] M. Montero Carrero, I. R. Sánchez, W. D. Paepe, A. Parente, and F. Contino, "Is There a Future for Small-Scale Cogeneration in Europe ? Economic and Policy Analysis of the Internal Humid Air Turbine Cycles," *Energies*, vol. 12, no. 3, pp. 1–27, 2019.

[18] B. Zakeri and S. Syri, "Electrical energy storage systems: A comparative life cycle cost analysis," *Renewable and sustainable energy reviews*, vol. 42, pp. 569–596, 2015.

[19] M. Di Somma, B. Yan, N. Bianco, G. Graditi, P. Luh, L. Mongibello, and V. Naso, "Multi-objective design optimization of distributed energy systems through cost and exergy assessments," *Applied Energy*, vol. 204, pp. 1299–1316, 2017.

[20] P. Balcombe, D. Rigby, and A. Azapagic, "Investigating the importance of motivations and barriers related to microgeneration uptake in the UK," *Applied Energy*, vol. 130, pp. 403–418, 2014.

[21] D. Coppitters, W. De Paepe, and F. Contino, "Surrogate-assisted robust design optimization and global sensitivity analysis of a directly coupled photovoltaic-electrolyzer system under techno-

economic uncertainty," *Applied Energy*, vol. 248, pp. 310–320, 2019.

[22] S. Giorgetti, D. Coppitters, F. Contino, W. D. Paepe, L. Bricteux, G. Aversano, and A. Parente, "Surrogate-Assisted Modeling and Robust Optimization of a Micro Gas Turbine Plant With Carbon Capture," *Journal of Engineering for Gas Turbines and Power*, vol. 142, no. 1, 2020.

[23] Elia, "Electricity scenarios for Belgium towards 2050: Eliaś quantified study on the energy transition in 2030 and 2040," Elia, Tech. Rep., 2017.

[24] D. Devogelaer, D. Gusbin *et al.*, "Working Paper 03-15-2030 Climate and Energy Framework for Belgium-Impact assessment of a selection of policy scenarios up to 2050," Federal Planning Bureau, Tech. Rep., 2015.

[25] D. Thomas, D. Mertens, M. Meeus, W. Van der Laak, and I. Francois, "Power-to-Gas Roadmap for Flanders," WaterstofNet, Tech. Rep., 2016.

[26] I. Duić, N. Štefanić, Z. Lulić, G. Krajačić, T. Pukšec, and T. Novosel, "EU28 fuel prices for 2015, 2030 and 2050. Deliverable 6.1: Future fuel price review," 2017.

[27] T. Nyoni, "Time series modeling and forecasting of the consumer price index in belgium," *Munich Personal RePEc Archive*, 2019.

[28] S. Abraham, M. Raisee, G. Ghorbaniasl, F. Contino, and C. Lacor, "A robust and efficient stepwise regression method for building sparse polynomial chaos expansions," *Journal of Computational Physics*, vol. 332, pp. 461–474, 2017.